sustainability

Article

Evaluation of Satellite-Based and Reanalysis Precipitation Datasets with Gauge-Observed Data over Haraz-Gharehsoo Basin, Iran

Mohammad Reza Goodarzi [1], Roxana Pooladi [2] and Majid Niazkar [3,*]

[1] Department of Civil Engineering, Yazd University, Yazd 8915813135, Iran
[2] Department of Civil Engineering, Water and Hydraulic Structures, Ayatollah Ozma Borujerdi University, Borujerd, Iran
[3] Department of Agricultural and Environmental Sciences, University of Milan, Via Celoria 2, 20133 Milan, Italy
* Correspondence: majid.niazkar@unimi.it

Abstract: Evaluating satellite-based products is vital for precipitation estimation for sustainable water resources management. The current study evaluates the accuracy of predicting precipitation using four remotely sensed rainfall datasets—Tropical Rainfall Measuring Mission products (TRMM-3B42V7), Precipitation Estimation from Remotely Sensed Information using Artificial Neural Networks Climate Data Records (PERSIANN-CDR), Cloud Classification System-Climate Data Record (PERSIANN-CCS-CDR), and National Centers for Environmental Prediction (NCEP)-Climate Forecast System Reanalysis (CFSR)—over the Haraz-Gharehsoo basin during 2008–2016. The benchmark values for the assessment are gauge-observed data gathered without missing precipitation data at nine ground-based measuring stations over the basin. The results indicate that the TRMM and CCS-CDR satellites provide more robust precipitation estimations in 75% of high-altitude stations at daily, monthly, and annual time scales. Furthermore, the comparative analysis reveals some precipitation underestimations for each satellite. The underestimation values obtained by TRMM CDR, CCS-CDR, and CFSR are 8.93 mm, 20.34 mm, 9.77 mm, and 17.23 mm annually, respectively. The results obtained are compared to previous studies conducted over other basins. It is concluded that considering the accuracy of each satellite product for estimating remotely sensed precipitation is valuable and essential for sustainable hydrological modelling.

Keywords: satellite-based products; gauge-observed data; TRMM; CDR; CCS-CDR; CFSR

check for updates

Citation: Goodarzi, M.R.; Pooladi, R.; Niazkar, M. Evaluation of Satellite-Based and Reanalysis Precipitation Datasets with Gauge-Observed Data over Haraz-Gharehsoo Basin, Iran. *Sustainability* **2022**, *14*, 13051. https://doi.org/10.3390/su142013051

Academic Editor: Ozgur Kisi

Received: 25 August 2022
Accepted: 6 October 2022
Published: 12 October 2022

1. Introduction

Estimating precipitation is vital for sustainable water resource management, hydrological modelling, and rainfall-trigged hazard forecasting [1]. For instance, fine-grained hydrological models require the reliable spatiotemporal distribution of precipitation, as one of the most impactful hydroclimatic input variables [2–4]. Rainfall variations significantly affect topographic and climatic conditions and water resource systems [5]. Furthermore, precipitation is the most significant section of the water cycle balance [6] and the primary input of hydrological models, and these data can be used to evaluate water resource management and climate change [7]. Thus, estimating precipitation helps simulate hydrological cycles in a study area [8].

Adopting a reliable method for estimating precipitation has always been an important and controversial issue. In essence, three major approaches for measuring/estimating precipitation are (1) gauge-observed data, (2) remotely sensed data, and (3) weather radar observations [9]. Among these methodologies, obtaining high-quality ground precipitation data for hydrological modelling is challenging [10,11], and hence, remotely sensed rainfall products are far more preferred for hydrometeorological applications.

One of the most significant advantages of satellite-based data against observed data is broader coverage worldwide. Comparing the remotely sensed data with ground observations is necessary for assessing the accuracy of estimations obtained by satellite-based rainfall data [9]. The remotely sensed rainfall estimates have exhibited strong rain-rate dependency [12]. A dense network of gauges and ground stations is essential to obtain acceptable precipitation data and climatic conditions [13,14]. The rainfall data are obtained from a terrain gauge-observed precipitation network; these inputs are always challenging because of the uneven and sparse distribution of in situ precipitation stations, limited time scales and retrieval errors [15–19]. In general, since there are no rain gauges in highlands and impassable areas, the accurate estimation of rainfall data is essential for compensating for the lack of ground gauge-observed data [20,21]. The dispersion of precipitation gauges, especially in inaccessible and mountainous areas, causes inaccurate hydrological forecasts [22]. Therefore, the operation of remotely sensed products must be considered for a specific and peculiar region before using these data [23]. Since meteorological and hydrometer stations do not exist in many areas, including highlands and impassable areas, the importance of the precise evaluation and estimation of remote-sensing rainfall data and the realisation of the water cycle by using remote-sensing and satellite-based precipitation methods has become more visible. As a result, estimating precipitation using remotely sensed data has been of utmost importance, mainly where ground-based measuring stations are scarce.

The rapid growth of remote sensing could help generating high-quality satellite-based precipitation data [24]. High-resolution satellite-based products are now frequently employed for hydrological modelling. Tropical Rainfall Measuring Mission (TRMM) Multi-satellite Precipitation Analysis (TEMPA) [25], Climate Prediction Center (CPC) morphing algorithm (CMORPH) [26], Tropical Applications of Meteorology using SATellite (TAMSAT) [27,28], National Centers for Environmental Prediction (NCEP)-Climate Forecast System Reanalysis (CFSR), the Precipitation Estimation from Remotely Sensed Information using Artificial Neural Networks-Climate Data Record (PERSIANN-CDR) [29–31], Precipitation Estimation from Remotely Sensed Information using Artificial Neural Networks-Cloud Classification System-Climate Data Record (PERSIANN-CCS-CDR) [32], and African Rainfall Climatology [33] are some satellite-based products widely used in precipitation studies.

Among various satellite-based products for precipitation analysis, the TRMM-3B42V7, PERSIANN-CDR, and PERSIANN-CCS-CDR are the most broadly used ones as they provide the best extensive performance owing to their high temporal and spatial resolution. Moreover, to better compare precipitation data, reanalysis-based data (CFSR) are chosen. The background literature has reported improvement in these versions compared to the previous versions. Few studies have evaluated the accuracy and performance of satellite-based precipitation products against gauge-observed data in Iran. According to the literature, Darand et al. [34] assessed the performance of TEMPA estimation in Iran, concluding that precipitation's spatial and temporal variations are well captured. Javanmard et al. [35] employed a high-resolution gridded rainfall dataset by satellite precipitation estimates of TRMM-3B42 over Iran. The results illustrated that the TRMM products agree well with the benchmark rainfall pattern. Despite previous studies, further investigations are required to compare satellite-based precipitation datasets with gauge-observed data, especially in regions with scarce ground-based observation data.

This study aims to excel at the inter-comparison of the remote-sensing products by analysing the error characteristics of TRMM, CDR, CCS-CDR, and CFSR precipitation products at the Haraz-Gharehsoo basin. This area is one of the most critical watersheds in Iran as it is constantly exposed to floods and erosion. Moreover, the primary meteorological phenomenon in the area under investigation is rainfall, which can cause natural disasters. This study measures precipitation phenomena in some critical coordinates of ground stations to determine their remotely sensed precipitation product's accuracy against gauge-observed data and follows these steps: First, the precipitation products are evaluated using several indicators based on the proper temporal scale in this basin. Subsequently, a correlation method and modified data are developed to improve the quality of satellite precipitation products and the error decomposition of TRMM products, evaluate statistical parameters for the basin in temporal and spatial scales, consider an error-component method, and finally choose the best satellite-based products for the Haraz-Gharehsoo basin.

2. Materials and Methods

2.1. Study Area

The Caspian basin is located in the north of Iran and has seven sub-basins, one of which is Haraz-Gharehsoo. It is located on the southern shores of the Caspian Sea and Gorgan Bay. The Haraz River and all of the rivers located in the area are known as the Haraz-Gharehsoo basin. The rivers are located at the northern foot of the Central Alborz mountains and extend from Haraz (Mahmoodabad) to Bandar-E-Gaz. The total area of the basin is 18644 km^2, and the geographical coordination is between 51°26′ E to 54°44′ E and 35° 45′ N to 36°10′ N. The geographical features and the spatial distribution of the nine stations of the Haraz-Gharehsoo basin are shown in Figure 1. The western part of this basin has a humid Mediterranean climate, whereas the eastern region has a semi-arid and humid climate.

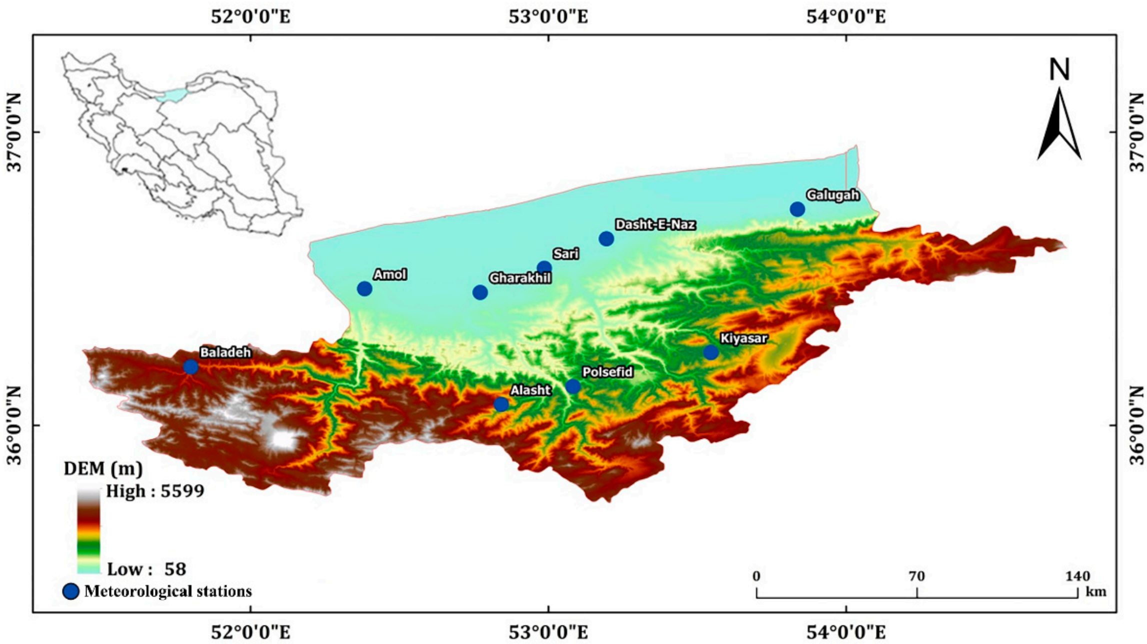

Figure 1. The spatial distribution of gauge-observed stations and a topographic map of the Haraz-Gharehsoo basin.

Table 1 shows the average precipitation on daily, monthly, and annual scales. The mean annual temperature is 15.5 °C and the mean annual precipitation is 597.3 mm, as summarised in Table 1. The geographical characteristics of the Haraz-Gharehsoo basin are shown in Table 2.

Table 1. Average precipitation amounts on daily, monthly and annual scales in the Haraz-Gharehsoo basin (unit: mm).

Datasets	Daily	Jan	Feb	Mar	Apr	May	June	July	Aug	Sep	Oct	Nov	Dec	Annual
Gauge-Observed	1.64	55.1	70.7	62.5	32.3	20.4	29.6	26.9	32.4	61.3	78.8	69.8	57.5	597.3
TRMM	1.38	45.6	59.1	48.5	34.1	24.1	23.8	22.4	26.3	52.7	52.2	63.3	44.6	496.7
CDR	0.96	34.9	43.2	39.2	31.6	18.7	12.2	9.7	10.8	28.7	44.5	39.9	35.9	349.3
CFSR	1.12	34.7	40.9	42.6	33.9	32.7	29.1	15.3	19.9	20.1	40.5	46.7	34.1	390.5
CCS-CDR	1.31	54.2	65.7	60.7	48.9	28.9	13.5	3.5	4.2	25.2	54.9	61.7	48.9	470.3

Table 2. Geographical characteristics of the Haraz-Gharehsoo basin.

Name	Longitude (°E)	Latitude (°N)	Elevation (m)
Sari	52.98	36.53	23
Baladeh	51.8	36.2	2120
Galugah	53.83	36.73	−10
Gharakhil	52.77	36.45	14.7
Kiyasar	53.54	36.24	1294.3
Alasht	52.84	36.07	1805
Amol	52.38	36.46	23.7
Polsfid	53.08	36.13	610
Sari (Dasht-E- Naz airport)	53.19	36.63	16.7

2.2. Data Sets

2.2.1. Basic and Gauge-Observed Data

The primary datasets used in this study are the daily meteorological and hydrometeorological data (2008–2016) obtained from the Iran Meteorological Organization. These data include average relative humidity, average temperature, daily minimum and maximum temperature and the daily, monthly, and annual precipitation data of nine meteorological stations (https://data.irimo.ir/ accessed on 1 April 2022). There are no missing data during the nine-year study period. To access reliable results, nine stations were chosen with different topographical conditions. All the gauges are distributed homogeneously in the Haraz-Gharehsoo basin, which is helpful for rainfall detection. The 30 m resolution Digital Elevation Model (DEM) is downloaded from https://earthexplorer.usgs.gov/ accessed on 1 April 2022.

2.2.2. Remote Sensing Precipitation Data

The TRMM is a collaboration between the National Aeronautics and Space Administration (NASA) and Japan's National Space Development Agency (JAXA) to observe and study tropical and subtropical precipitation. The TRMM satellite has been in operation since 1998. This satellite is broadly used with perfect performance because of the high spatial and temporal resolution and dependable inversion algorithm. The TRMM satellite is available for use 10 to 15 days after the end of each month. The TRMM provides important precipitation information using several space-borne instruments to increase the realisation of interaction between clouds, precipitation, and water vapour. The spatial and temporal resolutions of TRMM are 0.25° and daily, respectively. Moreover, the TRMM's coverage is global, ranging from 50° S to 50° N (http://disc.gsfc.nasa.gov/ accessed on 1 April 2022).

The PERSIANN-CDR provides daily rainfall estimates at a spatial resolution of 0.25° in the latitude band 60° S–60° N. These data are available from March 2000 to the present (http://chrsdata.eng.uci.edu accessed on 1 April 2022). As explained by the United States National Research Council Committee, CDR is a time series of measurements of sufficient length, consistency, and continuity measurements to determine climate change and variability. NASA and the National Oceanic Atmospheric Administration (NOAA) have sponsored operational and grant programs to create CDRs. PERSIANN-CCS-CDR provides 3-hourly precipitation estimates at a spatial resolution of 0.04° in the latitude band 60° S–60° N. The PERSIAN-CDR and PERSIANN-CCS-CDR products are available on these websites, http://chrsdata.eng.uci.edu accessed on 1 April 2022 and http://ncei.noaa.gov/products/climate-data-records accessed on 1 April 2022.

The CFSR data is a reanalysis product developed by NOAA that has global coverage. This product is available from 1979 to 2014 and the spatial and temporal resolution of CFSR is 38 km and daily, respectively. CFSR data are available at https://cfs.ncep.noaa.gov/cfsr/downloads/ accessed on 1 April 2022. A list of the details of satellite rainfall data (TRMM-3B42V7, PERSIANN-CDR, PERSIANN-CCS-CDR, and CFSR) is shown in (Table 3).

Table 3. Data description and characteristics of rainfall datasets.

Datasets	Name	Spatial Resolution	Temporal Resolution	Period	Coverage
TRMM-3B42V7	TRMM	0.25°	Daily	2008–2016	50° S–50° N
PERSIANN-CDR	CDR	0.25°	Daily	2008–2016	60° S–60° N
NCEP-CFSR	CFSR	38 km	Daily	2008–2014	labolG
PERSIANN-CCS-CDR	CCS-CDR	0.04°	3-hourly	2008–2016	60° S–60° N
Gauge-Observed	OBS	Point	Daily	2008–2016	Haraz-Gharehsoo Basin

2.3. Methodology

2.3.1. Data Preparation and Technical Framework

In this study, the gauge-observed data with no missing values are considered for testing the satellite-based products. Daily data create monthly and annual precipitation data for assessing the performance of precipitation products [1]. To better evaluate remotely sensed rainfall data, the nearest neighbour of the gridded data is chosen to fit the data and interpolate the gridded data from the remote sensing data grids to determine the weather station's location. CCS-CDR data are obtained from equations 9 to 11. In the first step, the data values are compared to the gauge-observed data. The second step is to assess the rainfall dataset and examine the utilisation of the satellite-based rainfall dataset in the specific points against gauge-observed data. Afterwards, some statistical metrics are exploited in spatial and temporal periods in the Haraz-Gharehsoo basin to check the accuracy of the satellite-based data. In the subsequent stage, the TRMM data errors are identified and corrected using a correlations model between TRMM and OBS data from April to September, while the precision of data is considered by the error-component method. For more scrutiny of the accuracy evaluation of satellite-based data, the statistical metrics are calculated for daily precipitation intensity (PI) [36].

2.3.2. Evaluation of Statistical Metrics

Some of the statistical metrics that are used to consider the satellite-based accuracy in the Haraz-Gharehsoo basin include Mean Error (ME), Root Mean Square Error (RMSE), Percentage Bias (PBIAS), Correlation Coefficient (CC), Probability of Detection (POD), False Alarm Ratio (FAR), Critical Success Index (CSI) [37,38], and Bias in Detection (BID) [39]. The statistical metrics used in this study are shown in Table 4. The optimal values of ME, RMSE, PBIAS and FAR are 0, and the optimal values of CC, POD, CSI, BID and HSS are 1 [40]. The BID represents the inclination to overestimate (BID > 1) or underestimate (BID < 1) [39].

Table 4. Statistical metrics used for evaluating satellite-based precipitation estimations.

Number	Abbreviation	Definition	Unit	Function	Description
(1)	ME	Mean Error	mm	$\mathrm{ME} = \frac{1}{n}\sum_{i=1}^{n}(S_i - G_i)$	G_i: Gauge-observed precipitation.
(2)	RMSE	Root Mean Square Error	mm	$\mathrm{RMSE} = \sqrt{\frac{1}{n}\sum_{i=1}^{n}(S_i - G_i)}^2$	S_i: Precipitation that is driven by satellite-based products.
(3)	PBIAS	Percentage Bias	%	$\mathrm{PBIAS} = \frac{\sum_{i=1}^{n}(S_i - G_i)}{\sum_{i=1}^{n}G_i} \times 100\%$	H: Correct detection of the observed rainfall.
(4)	CC	Correlation Coefficient		$\mathrm{CC} = \frac{\sum_{i=1}^{n}(G_i - \overline{G})(S_i - \overline{S})}{\sqrt{\sum_{i=1}^{n}(G_i - \overline{G})^2}.\sqrt{\sum_{i=1}^{n}(S_i - \overline{S})^2}}$	M: The observed rainfall is not detected.
(5)	POD	Probability Of Detection		$\mathrm{POD} = \frac{H}{H+M}$	F: The rainfall is detected but not observed.
(6)	FAR	False Alarm Ratio		$\mathrm{FAR} = \frac{F}{H+F}$	$\overline{G} = \frac{1}{n}\sum_{i=1}^{n}G_i$
(7)	CSI	Critical Success Index		$\mathrm{CSI} = \frac{H}{H+M+F}$	$\overline{S} = \frac{1}{n}\sum_{i=1}^{n}S_i$
(8)	BID	Bias In Detection		$\mathrm{BID} = \frac{H+F}{H+M}$	$r_{PERSIANN-CCS}$: 30 min/3-hourly PERSIANN-CCS estimate (0.04° spatial resolution) i: Latitude of the 30 min/3-hourly PERSIANN-CCS at 0.04° × 0.04°.

Table 4. *Cont.*

Number	Abbreviation	Definition	Unit	Function	Description
(9)	$R_{\text{Cum-PERSIANN-CCS}}$ (i′, j′)	Monthly 2.5° aggregated PERSIANN-CCS estimate		$R_{\text{Cum-PERSIANN-CCS}}$ (i′, j′) = $\sum_0^{nd}\sum_0^{nh}\left(\sum_0^{62}\sum_0^{62}[r_{PERSIANN-CCS}(i,j]\right) \geq thd$	j: Longitude of the 30 min/3-hourly PERSIANN-CCS at 0.04° × 0.04°.
(10)	w (i′, j′)	Bias adjustment weights for each monthly 2.5° grid cell		w (i′, j′) = R_{CDR} (i′, j′)/$R_{\text{Cum-PERSIANN-CCS}}$ (i′, j′) $0 \leq w \leq 2.5$	i′: Latitude of the aggregated PERSIANN-CCS at 2.5° × 2.5°.
(11)	PERSIANN-CCS-CDR (i, j)	Final PERSIANN-CCS-CDR product		$\text{PERSIANN}-\text{CCS}-\text{CDR}\ (i,\ j) = w(i,\ j) \times r_{PERSIANN-CCS}(i,\ j)$	j′: Longitude of the aggregated PERSIANN-CCS at 2.5° × 2.5°.

3. Results and Discussion

3.1. Comparison and Evaluation of Satellite-Based Precipitation Data against Gauge-Observed Products

The average remotely sensed precipitation values are calculated for different time scales (i.e., daily, monthly, and annual) at nine stations in the Haraz-Gharehsoo basin for the 9-year period from 2008 to 2016. The coordinates of ground and satellite-based stations are considered precisely at the same points to determine the precision of remotely sensed precipitation products against gauge-observed stations. The average monthly and yearly precipitation data calculated for nine stations are shown in Figure 2. As shown, the rainfall events have been well captured by TRMM and CCS-CDR, and the values of both remote sensing rainfall products follow almost the same precipitation trend as the OBS data on the monthly scale. However, the plot demonstrates that underestimations exist with the gauge-observed data, which has consistency with other studies [41].

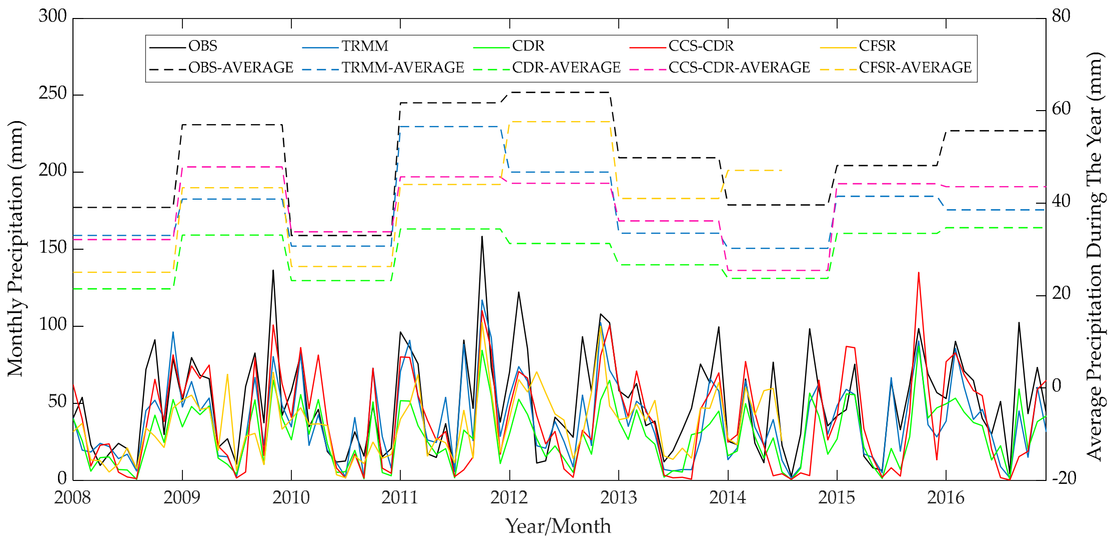

Figure 2. Comparison of the average monthly precipitation in the Haraz-Gharehsoo basin at nine stations with solid lines and during the year with dashed lines.

According to Figure 2, the CDR and CFSR satellite is not very suitable for the Haraz-Gharehsoo basin. To be more specific, the CDR precipitation data has the poorest performance on the monthly scale among the other satellites (matching results are found in [42]). All of the remote-sensing datasets have underestimations [43]. Moreover, TRMM, CDR, CCS-CDR, and CFSR have underestimated precipitation data in this basin, but the underestimation of CDR is greater than the other products. The underestimation of the average precipitation data by TRMM, CDR, CCS-CDR, and CFSR satellites on the monthly scale is 8.93 mm, 20.34 mm, 9.77 mm, and 17.23 mm, respectively. Additionally, the trend of TRMM data is more similar to gauge-observed data. The similarity of the trend of TRMM and CCS-CDR rainfall data is more visible on the monthly and annual scales. Overall, the satellite rainfall data demonstrated higher adaptability with gauge-observed data in producing monthly precipitation.

The adaptability of all the rainfall products increases from daily to monthly and annual resolutions, which is compatible with previous studies [44]. One of the reasons that the TRMM data yielded more robust estimations than CDR is that the former has Special Sensor Microwave Imager/Sounder (SSMIS) sensor data that provides more high-quality passive microwave data. This significantly improves the accuracy of TRMM precipitation [3].

The cumulative diagram of monthly precipitation data for OBS, TRMM, CDR, CCS-CDR, and CFSR data from 2008 to 2016 in the Haraz-Gharehsoo Basin is shown in Figure 3. The slope of the curve indicates the estimated deviation of the total cumulative monthly precipitation. According to Figure 3, the deviation of CDR precipitation data against OBS is more than the other datasets. As of May 2013, CDR, TRMM, CCS-CDR, and CFSR were underestimated by 1976.8 mm, 1080 mm, 1190 mm, and 1761 mm, respectively. Generally, TRMM has a small degree of deviation against OBS.

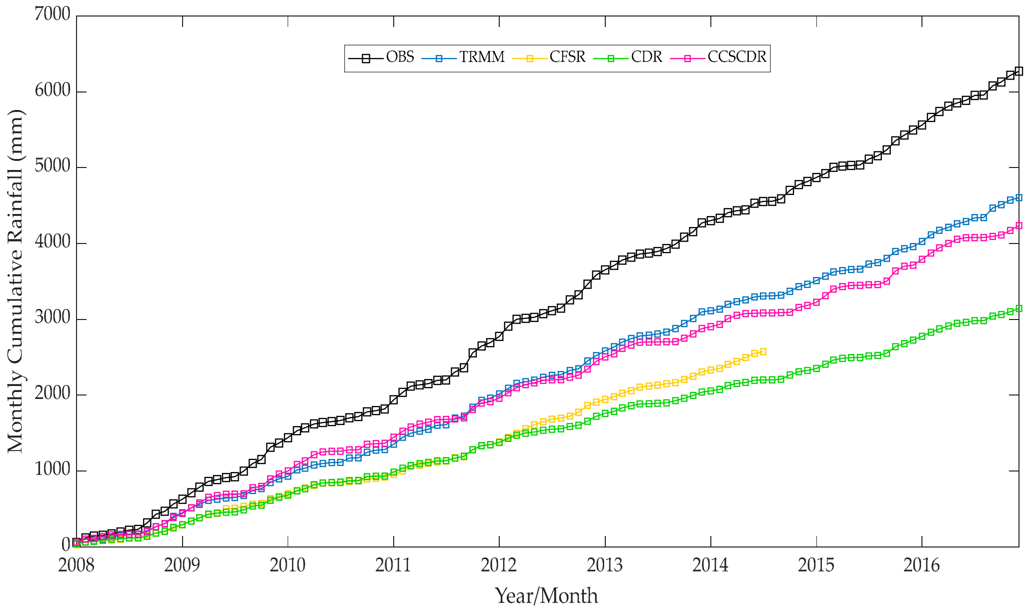

Figure 3. Comparison of total cumulative rainfall on a monthly scale at nine stations in the Haraz-Gharehsoo basin.

As shown in Table 1, the difference in average daily precipitation between the TRMM and gauge-observed data is less than CDR, CCS-CDR, and CFSR. The difference in average daily precipitation between TRMM, CDR, CCS-CDR, and CFSR against gauge-observed data is 0.26 mm, 0.68 mm, 0.33 mm, and 0.52 mm, respectively. According to the data in Table 1, TRMM precipitation products have a minor difference with gauge-observed data from April to September, and the differences between the average annual precipitation of TRMM, CDR, CCS-CDR, and CFSR against gauge-observed data are 100.6 mm, 248 mm, 127 mm, and 206.8 mm, respectively.

The CC, RMSE, ME, and PBIAS values were calculated for different stations and PI levels at different time scales. The CC and RMSE for TRMM, CDR, CCS-CDR, and CFSR products in the Haraz-Gharehsoo basin are illustrated in Figure 4. According to Figure 4a, CC and RMSE values for TRMM in the Haraz-Gharehsoo Basin on a daily scale are 0.71 and 0.65 mm, respectively. As shown in Figure 4b, the corresponding values are 0.52 and 0.68 mm for the CDR satellite on a daily scale. As demonstrated in Figure 4c,d, the CC and RMSE values for CCS-CFSR, and CFSR values are 0.71, 0.75 mm, 0.50, and 0.53 mm, respectively. According to Figure 4, TRMM satellite-based data perform better than the data on a daily scale.

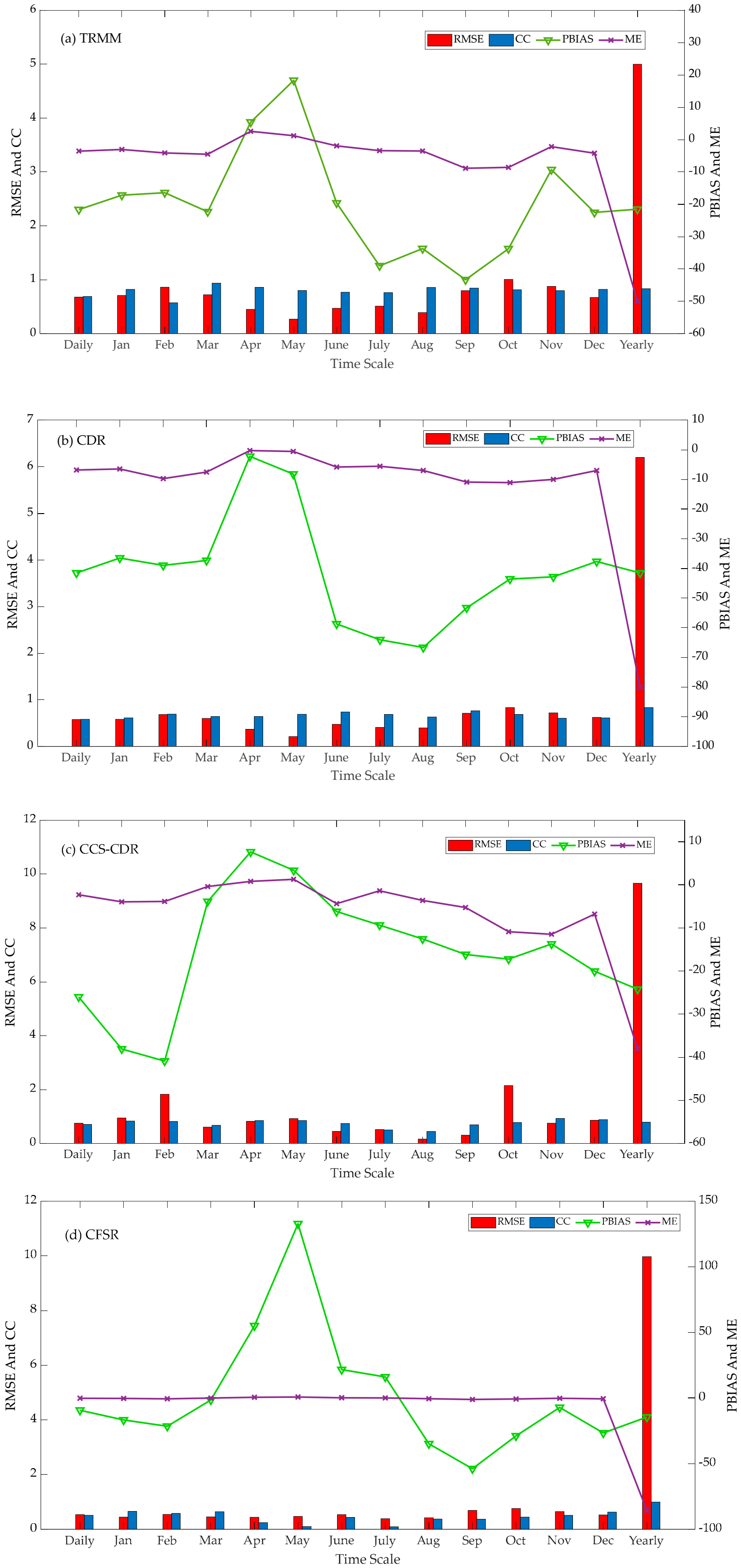

Figure 4. Comparison of the average precipitation metrics for satellite-based data at daily, monthly, and annual time scales in the Haraz-Gharehsoo basin: (**a**) TRMM, (**b**) CDR, (**c**) CCS-CDR, and (**d**) CFSR.

Table 5 illustrates the accuracy of the rainfall detection for each satellite based on a daily scale from the 1st of January 2008 to the 31st of July 2014. The POD demonstrates the ability of rainfall data to precisely record the actual precipitation event. The POD value of TRMM is the maximum, one being 0.51, followed by CDR, where the POD value is 0.39. FAR illustrates that the precipitation data wrongly predict the actual rainfall event. Moreover, CSI shows a false prediction of precipitation and reflects the capability of the rainfall data to detect actual precipitation occurrence. The BID shows the tendency to underestimate (BID < 1) or overestimate (BID > 1) the number of rainfall events, and the optimal value of BID is 1. The results demonstrate that the TRMM can detect rainfall occurrence better than others. The FAR, CSI, BID, and POD of the TRMM are 0.42, 0.71, 0.82, and 0.51, respectively.

Table 5. Precipitation detection capability in the Haraz-Gharehsoo basin.

Satellite	POD	FAR	BID	CSI
TRMM	0.51	0.42	0.82	0.71
CDR	0.39	0.25	0.93	0.54
CCS-CDR	0.45	0.34	0.86	0.59
CFSR	0.42	0.17	0.95	0.53

In general, both the TRMM and CCS-CDR satellites are more successful at high altitudes rather than the other satellites. Despite the different magnitudes of PBIAS in each station, the CDR satellite-based products demonstrated considerable underestimations in the study area. In contrast, TRMM products are more reliable in the Haraz-Gharehsoo basin. To further investigate the quality of satellite-based data in the Haraz-Gharehsoo basin, they were divided into six groups according to the daily PI. The classification results are depicted in Figure 5 from 2008 to 2016. The results of CDR satellites are overestimated in [0, 2) and [2, 5) and underestimated in other PI ranges. In addition, the TRMM performs well in a range of [0, 2) and has a similar trend to the observed data in other ranges. However, the precipitation amounts have been underestimated by the TRMM in all PI ranges.

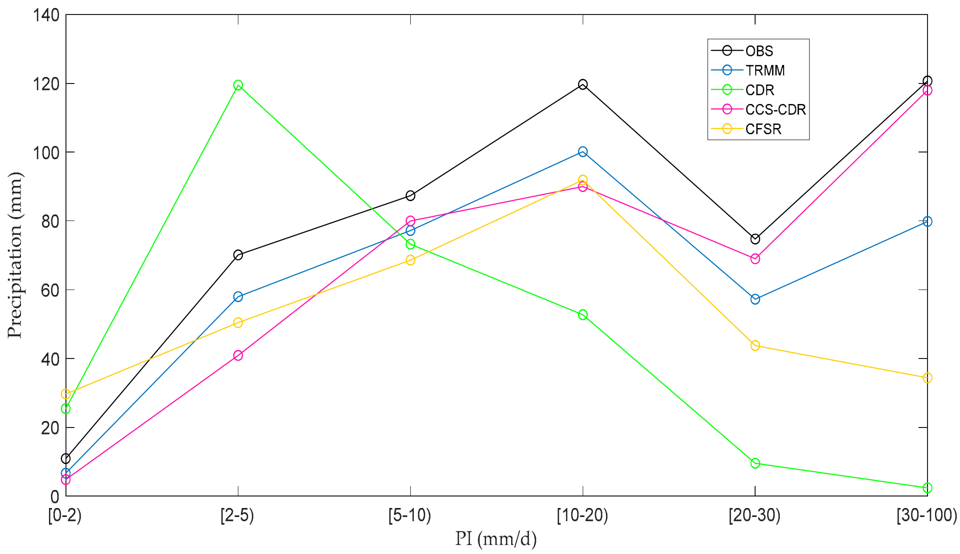

Figure 5. The average amount of precipitation products under different PI groups.

The TRMM underestimations in the PI range of [30, 100) related to heavy precipitation are higher than those of other PI intervals. The TRMM underestimation value in the range of [30, 100) was 40.8 mm. These products cannot demonstrate the ability of precipitation detection directly, while the CCS-CDR performs well with heavy precipitation [30, 100). So, to further explore the precision of remotely sensed rainfall data, the CC, RMSE, ME, and PBIAS values are calculated under different precipitation intensities (PI groups) for all satellites and are shown in Table 6. The correlation between OBS data and TRMM products in [5, 10) with CC = 0.876 and RMSE = 0.336 mm is higher than in the other intervals. Obviously, RMSE is enhanced by increasing the precipitation intensity. On the other hand, the CDR products have the weakest performance in [30, 100) by CC = 0.004 and RMSE = 4.625 mm. The CCS-CDR has the best CC with heavy precipitation [30, 100); this CC value is 0.957, while for [0, 2) it has the least RMSE, equal to 0.045. According to Table 7, for the higher precipitation data range (≥0.1), the CCS-CDR performs better than the TRMM. Therefore, correcting the satellite data error based on the highest correlation between the satellite-based data is necessary.

Table 6. Statistical criteria of satellite-based precipitation datasets against observed data under various PI groups.

PI (mm/Day)	TRMM				CDR			
	CC	**RMSE (mm)**	**ME (mm)**	**PBIAS (%)**	**CC**	**RMSE (mm)**	**ME (mm)**	**PBIAS (%)**
[0,2)	0.060	0.018	−0.017	−39.054	0.122	0.028	0.061	133.059
[2, 5)	0.709	0.192	−0.404	−17.293	0.002	0.200	0.945	70.429
[5, 10)	0.876	0.336	−0.778	−11.598	0.119	0.345	−1.083	−16.125
[10, 20)	0.867	0.701	−2.274	−16.549	0.101	1.067	−7.702	−56.045
[20, 30)	0.795	1.205	−5.550	−23.398	0.457	2.225	−20.755	−87.213
[30, 100)	0.623	3.277	−14.960	−33.843	0.004	4.625	−43.332	−98.024
		CCS−CDR					**CFSR**	
	CC	**RMSE (mm)**	**ME (mm)**	**PBIAS (%)**	**CC**	**RMSE (mm)**	**ME (mm)**	**PBIAS (%)**
[0,2)	0.032	0.045	−0.258	−43.869	0.007	0.062	0.156	22.691
[2, 5)	0.377	0.369	−1.854	−12.483	0.353	0.315	2.922	28.646
[5, 10)	0.564	0.257	−0.212	−5.816	0.350	0.682	6.290	7.290
[10, 20)	0.687	0.153	−1.864	−14.267	0.349	1.320	12.010	26.576
[20, 30)	0.886	0.098	−6.427	−26.364	0.467	2.148	18.492	33.178
[30, 100)	0.957	0.754	−8.733	−37.125	0.397	8.961	21.621	51.178

Table 7. Comparison of observed data and satellite data at high and low precipitation.

	TRMM ≥ 0.1 mm/h	**TRMM < 0.1 mm/h**
OBS ≥ 0.1 mm/h	2471 (8.35%)	2968 (10.03%)
OBS < 0.1 mm/h	1030 (3.48%)	23123 (78.14%)
	CDR ≥ 0.1 mm/h	**CDR < 0.1 mm/h**
OBS ≥ 0.1 mm/h	2638 (8.92%)	3132 (10.58%)
OBS < 0.1 mm/h	866 (2.93%)	22956 (77.57%)
	CCS-CDR ≥ 0.1 mm/h	**CCS-CDR < 0.1 mm/h**
OBS ≥ 0.1 mm/h	2856 (9.65%)	3223 (10.89%)
OBS < 0.1 mm/h	923 (3.12%)	22590 (76.34%)
	CFSR ≥ 0.1 mm/h	**CFSR < 0.1 mm/h**
OBS ≥ 0.1 mm/h	2722 (12.58%)	2465 (11.39%)
OBS < 0.1 mm/h	416 (1.93%)	16033 (74.1%)

3.2. Error Decomposition of TRMM Products

By virtue of the good performance of the TRMM data, especially from April to September, the satellite data were corrected by creating a correlation model between TRMM and OBS data. To correct the satellite-based data errors, in the first step, a scatter plot was drawn between the satellite-based products and the OBS in the wet season in the Haraz-Gharehsoo basin. After drawing the scatter plot, the linear fit between satellite-based products and OBS was obtained as the trend line equation. In the next step, the satellite-based datasets were corrected according to the correlation model. The scatter plot of the satellite-based and OBS precipitation products is shown in Figure 6a–c. Thus, the error of the satellite-based datasets is minimised for the Haraz-Gharehsoo basin. The data obtained by error correction were called corrected data. In order to evaluate the quality of the corrected datasets, the CC, ME, RMSE, and PBIAS values were computed on daily, monthly, and annual scales for the Haraz-Gharehsoo basin, and the corresponding results are depicted in Figure 7a–c. Due to obtaining this method for correcting satellite-based products, the accuracy of the data improved significantly. The results of the satellite-based corrected data in Figure 7a–c demonstrate that the PBIAS of the corrected data for TRMM, CDR, and CCS-CDR decreased by 47.9%, 43.3%, and 38.6% from 2008 to 2016 on a daily scale, respectively.

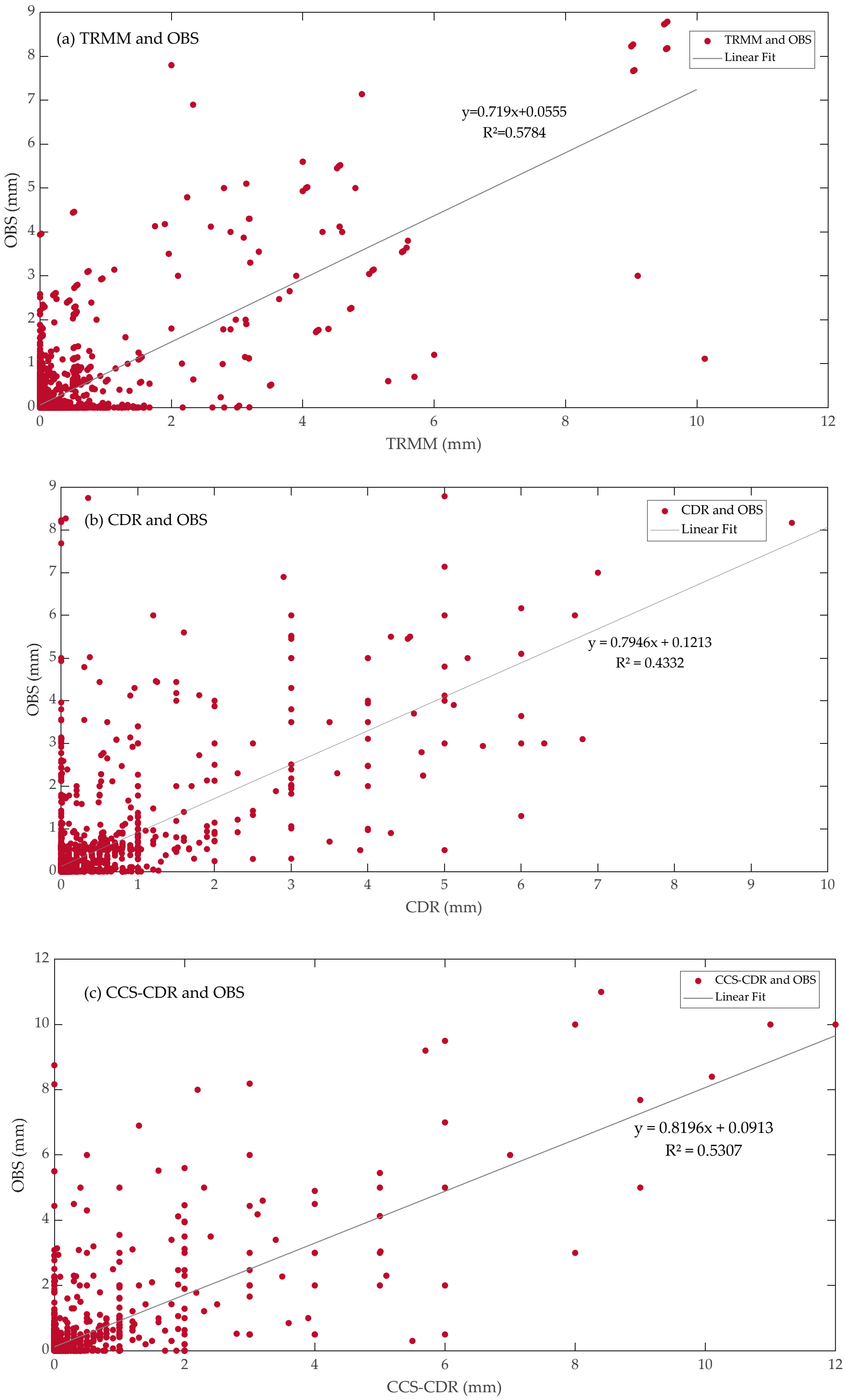

Figure 6. Scatter plot of the satellite-based and OBS precipitation products from April to September in the Haraz-Gharehsoo basin.

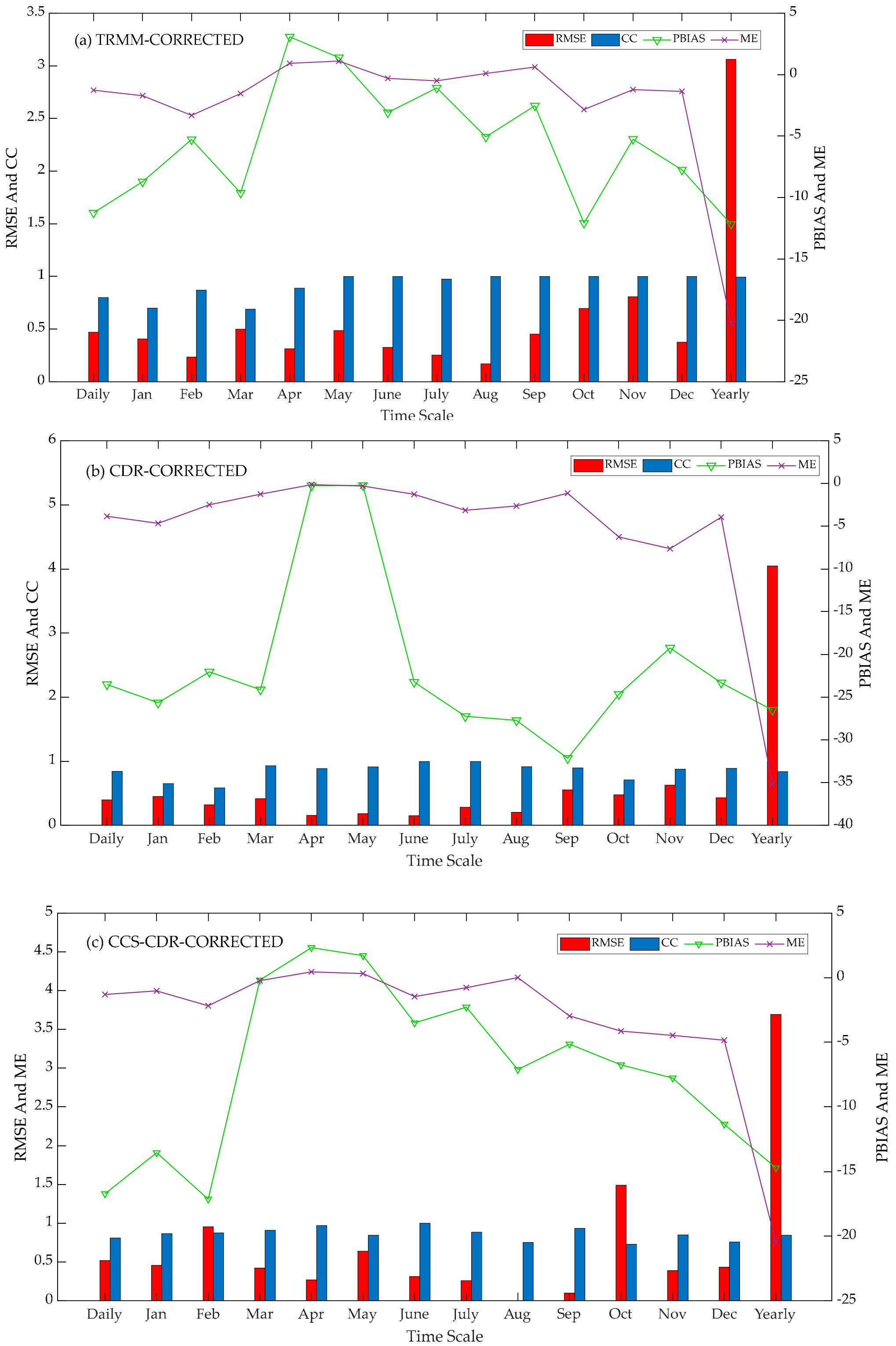

Figure 7. Comparison of the average precipitation metrics for (**a**) TRMM-CORRECTED, (**b**) CDR-CORRECTED, and (**c**) CCS-CDR-CORRECTED at different time scales in the Haraz-Gharehsoo basin.

The results illustrate that the data quality is enhanced and, consequently, the results are better than that of the TRMM, CDR, and CCS-CDR datasets. According to Figure 8 and Table 1, the average annual precipitation for TRMM, CDR, CCS-CDR, and CFSR products was underestimated by 16.85%, 41.52%, 21.26%, and 34.62% on an annual scale, respectively.

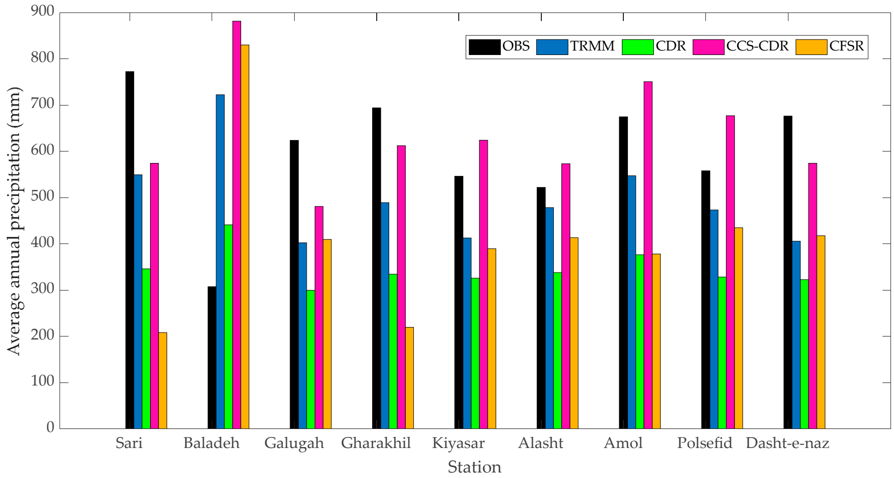

Figure 8. The average annual precipitation products in each station from 2008 to 2016.

Many factors affect the accuracy of satellite-based data, such as topography, altitude, geographical features, precipitation, and geological factors [45]. According to Figure 8, the TRMM performed poorly at Baladeh station in the southwest of the Haraz-Gharehsoo basin with an altitude of 2120 m and overestimated the average annual precipitation in the station. Because the satellites cannot detect some low-level clouds due to large cloudage and the complexity of the terrain in high-altitude regions, their retrieval accuracy is affected [46]. Estimations from satellite products can be used in high-altitude zones or areas with sparse stations [47].

The best estimation for the TRMM products was achieved at the Alasht station with an altitude of 1805 m. The average annual precipitation is the closest value to the observed data. The rate of underestimation at the Alasht station is only 8%. The CDR satellite-based products estimated the average annual precipitation better than the TRMM at Baladeh, while it underestimated the values at other stations. As shown in Figure 8, the TRMM and CCS-CDR performed better than the CDR and CCS on an annual scale. The TRMM performed relatively well in 75% of high-altitude points, such as Kiyasar, Alasht, and Polsefid, while only the Baladeh station has a 134% overestimation against the observed data.

4. Conclusions

This study evaluated the TRMM, CDR, CCS-CDR and CFSR satellite-based data in the Haraz-Gharehsoo basin. For this purpose, the position of the ground-based measuring stations at different altitudes was considered better to assess the performance of satellite products against gauge observations. The accuracy of the estimated data was evaluated by adopting statistical criteria, including CC, ME, RMSE, PBIAS, FAR, CSI, and BID at the whole basin and at each station on daily, monthly and annual time scales. Comparing the statistical metrics concluded that the CDR and CFSR satellite data are not helpful for the Haraz-Gharehsoo basin, as the corresponding data suffered a significant underestimation from 2008 to 2016. Therefore, the TRMM products were further investigated in light of finding an acceptable correlation against OBS. As a result, the data errors of satellite-based products were corrected and decomposed to provide corrected data. Considering the statistical metrics of corrected satellite-based data revealed that the improved data have fewer errors than that of the TRMM, CDR, and CCS-CDR. The main findings are as follows:

(1) Four remote sensing products evaluated in this study generally have an underestimation trend, while the TRMM and CCS-CDR products have better performance.
(2) The rainfall amounts of satellite-based products were examined precisely at the coordinates of gauge-observed stations by interpolating the data to assess the accuracy of satellite-based data better.

(3) Four of the TRMM, CDR, CCS-CDR, and CFSR products underestimate precipitation on daily, monthly, and annual scales, while the underestimations of CDR and CFSR are more remarkable than that of TRMM and CCS-CDR.
(4) Comparing the satellite products showed that the former performed better than the latter from April to September.
(5) By constructing the decomposition data error model, the CC, ME, RMSE, and PBIAS became closer to optimal values, especially on daily and monthly scales.
(6) On the diurnal scale, TRMM has the best precision for detecting rainfall occurrences, with CSI 0.71, followed by CCS-CDR, CDR, and CFSR. Moreover, TRMM, with a POD of 0.51, has a powerful capability to make reliable rainfall estimations.
(7) By comparing the precipitation intensity for TRMM and other products, it was found that the TRMM data has optimal statistical values when the PI range is [5, 10) by CC = 0.876 and RMSE 0.336 mm. Additionally, the worst performance belongs to CDR products in the PI range of [20, 30) by CC = 0.004 and RMSE = 4.625. This implies that the TRMM estimation is closer to OBS.
(8) CCS-CDR provides more accurate results than CDR products.

Due to the effect of multiple factors, such as topographic and climatic conditions on satellite-based products in different regions, it is suggested that the accuracy of satellite-based products is assessed in each region in favour of obtaining more robust results.

Author Contributions: Supervision, M.R.G.; design, and implementation of the research, M.R.G. and M.N.; analysis of the results, M.R.G. and R.P. and M.N.; the writing of the draft of the manuscript, M.R.G. and R.P.; modelling, R.P. and M.N.; writing, and revising the manuscript, M.N. All authors have read and agreed to the published version of the manuscript.

Funding: This research received no external funding.

Institutional Review Board Statement: Not applicable.

Informed Consent Statement: Not applicable.

Data Availability Statement: The data used for this study will be provided upon request.

Acknowledgments: The authors appreciate the Iran Meteorological Organization (IRIMO) for the support of data. We are grateful to the developers of the TRMM-3B42V7 and PERSIANN-CDR datasets for providing the data. The source of rainfall products utilized in this study is described in the article, and we will provide the data upon request.

Conflicts of Interest: The authors declare no conflict of interest.

References

1. Deng, P.; Zhang, M.; Bing, J.; Jia, J.; Zhang, D. Evaluation of the GSMaP_Gauge products using rain gauge observations and SWAT model in the Upper Hanjiang River Basin. *Atmos. Res.* **2019**, *219*, 153–165. [CrossRef]
2. Sharma, S.; Isik, S.; Srivastava, P.; Kalin, L. Deriving spatially distributed precipitation data using the artificial neural network and multilinear regression models. *J. Hydrol. Eng.* **2013**, *18*, 194–205. [CrossRef]
3. Yong, B.; Chen, B.; Gourley, J.J.; Ren, L.; Hong, Y.; Chen, X.; Wang, W.; Chen, S.; Gong, L. Intercomparison of the Version-6 and Version-7 TMPA precipitation products over high and low latitudes basins with independent gauge networks: Is the newer version better in both real-time and post-real-time analysis for water resources and hydrologic extremes? *J. Hydrol.* **2014**, *508*, 77–87.
4. Schwarzenbach, R.P.; Escher, B.I.; Fenner, K.; Hofstetter, T.B.; Johnson, C.A.; von Gunten, U.; Wehrli, B. The challenge of micropollutants in aquatic systems. *Science* **2006**, *313*, 1072–1077. [CrossRef] [PubMed]
5. Zahabiyoun, B.; Goodarzi, M.; Bavani, A.M.; Azamathulla, H.M. Assessment of climate change impact on the Gharesou River Basin using SWAT hydrological model. *CLEAN–Soil Air Water* **2013**, *41*, 601–609. [CrossRef]
6. Leta, O.T.; El-Kadi, A.I.; Dulai, H.; Ghazal, K.A. Assessment of climate change impacts on water balance components of Heeia watershed in Hawaii. *J. Hydrol. Reg. Stud.* **2016**, *8*, 182–197. [CrossRef]
7. Duarte, L.V.; Formiga, K.T.M.; Costa, V.A.F. Analysis of the IMERG-GPM Precipitation Product Analysis in Brazilian Midwestern Basins Considering Different Time and Spatial Scales. *Water* **2022**, *14*, 2472. [CrossRef]
8. Niu, P.; Zhang, E.; Feng, Y.; Peng, P. Spatial-Temporal Pattern Analysis of Land Use and Water Yield in Water Source Region of Middle Route of South-to-North Water Transfer Project Based on Google Earth Engine. *Water* **2022**, *14*, 2535. [CrossRef]

9. Liu, X.; Yang, T.; Hsu, K.; Liu, C.; Sorooshian, S. Evaluating the streamflow simulation capability of PERSIANN-CDR daily rainfall products in two river basins on the Tibetan Plateau. *Hydrol. Earth Syst. Sci.* **2017**, *21*, 169–181. [CrossRef]
10. Mekonnen, K.; Melesse, A.M.; Woldesenbet, T.A. Spatial evaluation of satellite-retrieved extreme rainfall rates in the Upper Awash River Basin, Ethiopia. *Atmos. Res.* **2021**, *249*, 105297. [CrossRef]
11. Acharya, S.C.; Nathan, R.; Wang, Q.J.; Su, C.-H.; Eizenberg, N. An evaluation of daily precipitation from a regional atmospheric reanalysis over Australia. *Hydrol. Earth Syst. Sci.* **2019**, *23*, 3387–3403. [CrossRef]
12. Tian, Y.; Peters-Lidard, C.D.; Adler, R.F.; Kubota, T.; Ushio, T. Evaluation of GSMaP precipitation estimates over the contiguous United States. *J. Hydrometeorol.* **2010**, *11*, 566–574. [CrossRef]
13. Duan, Z.; Tuo, Y.; Liu, J.; Gao, H.; Song, X.; Zhang, Z.; Yang, L.; Mekonnen, D.F. Hydrological evaluation of open-access precipitation and air temperature datasets using SWAT in a poorly gauged basin in Ethiopia. *J. Hydrol.* **2019**, *569*, 612–626. [CrossRef]
14. Kidd, C.; Becker, A.; Huffman, G.J.; Muller, C.L.; Joe, P.; Skofronick-Jackson, G.; Kirschbaum, D.B. So, how much of the Earth's surface is covered by rain gauges? *Bull. Am. Meteorol. Soc.* **2017**, *98*, 69–78. [CrossRef]
15. Li, D.; Christakos, G.; Ding, X.; Wu, J. Adequacy of TRMM satellite rainfall data in driving the SWAT modeling of Tiaoxi catchment (Taihu lake basin, China). *J. Hydrol.* **2018**, *556*, 1139–1152. [CrossRef]
16. Tong, K.; Su, F.; Yang, D.; Hao, Z. Evaluation of satellite precipitation retrievals and their potential utilities in hydrologic modeling over the Tibetan Plateau. *J. Hydrol.* **2014**, *519*, 423–437. [CrossRef]
17. Essou, G.R.; Sabarly, F.; Lucas-Picher, P.; Brissette, F.; Poulin, A. Can precipitation and temperature from meteorological reanalyses be used for hydrological modeling? *J. Hydrometeorol.* **2016**, *17*, 1929–1950. [CrossRef]
18. Ebert, E.E.; Janowiak, J.E.; Kidd, C. Comparison of near-real-time precipitation estimates from satellite observations and numerical models. *Bull. Am. Meteorol. Soc.* **2007**, *88*, 47–64. [CrossRef]
19. Xue, X.; Hong, Y.; Limaye, A.S.; Gourley, J.J.; Huffman, G.J.; Khan, S.I.; Dorji, C.; Chen, S. Statistical and hydrological evaluation of TRMM-based Multi-satellite Precipitation Analysis over the Wangchu Basin of Bhutan: Are the latest satellite precipitation products 3B42V7 ready for use in ungauged basins? *J. Hydrol.* **2013**, *499*, 91–99. [CrossRef]
20. Meng, J.; Li, L.; Hao, Z.; Wang, J.; Shao, Q. Suitability of TRMM satellite rainfall in driving a distributed hydrological model in the source region of Yellow River. *J. Hydrol.* **2014**, *509*, 320–332. [CrossRef]
21. Wang, N.; Yao, Z.; Liu, W.; Lv, X.; Ma, M. Spatial variabilities of runoff erosion and different underlying surfaces in the Xihe river basin. *Water* **2019**, *11*, 352. [CrossRef]
22. Li, X.; Long, D.; Han, Z.; Scanlon, B.R.; Sun, Z.; Han, P.; Hou, A. Evapotranspiration estimation for Tibetan Plateau headwaters using conjoint terrestrial and atmospheric water balances and multisource remote sensing. *Water Resour. Res.* **2019**, *55*, 8608–8630. [CrossRef]
23. Kimani, M.W.; Hoedjes, J.C.; Su, Z. An assessment of satellite-derived rainfall products relative to ground observations over East Africa. *Remote Sens.* **2017**, *9*, 430. [CrossRef]
24. Zhang, Y.; Ma, N. Spatiotemporal variability of snow cover and snow water equivalent in the last three decades over Eurasia. *J. Hydrol.* **2018**, *559*, 238–251. [CrossRef]
25. Huffman, G.J.; Bolvin, D.T.; Nelkin, E.J.; Wolff, D.B.; Adler, R.F.; Gu, G.; Hong, Y.; Bowman, K.P.; Stocker, E.F. The TRMM multisatellite precipitation analysis (TMPA): Quasi-global, multiyear, combined-sensor precipitation estimates at fine scales. *J. Hydrometeorol.* **2007**, *8*, 38–55. [CrossRef]
26. Joyce, R.J.; Janowiak, J.E.; Arkin, P.A.; Xie, P. CMORPH: A method that produces global precipitation estimates from passive microwave and infrared data at high spatial and temporal resolution. *J. Hydrometeorol.* **2004**, *5*, 487–503. [CrossRef]
27. Thorne, V.; Coakeley, P.; Grimes, D.; Dugdale, G. Comparison of TAMSAT and CPC rainfall estimates with raingauges, for southern Africa. *Int. J. Remote Sens.* **2001**, *22*, 1951–1974. [CrossRef]
28. Maidment, R.I.; Grimes, D.; Black, E.; Tarnavsky, E.; Young, M.; Greatrex, H.; Allan, R.P.; Stein, T.; Nkonde, E.; Senkunda, S.; et al. A new, long-term daily satellite-based rainfall dataset for operational monitoring in Africa. *Sci. Data* **2017**, *4*, 1–19.
29. Sorooshian, S.; Hsu, K.-L.; Gao, X.; Gupta, H.V.; Imam, B.; Braithwaite, D. Evaluation of PERSIANN system satellite-based estimates of tropical rainfall. *Bull. Am. Meteorol. Soc.* **2000**, *81*, 2035–2046. [CrossRef]
30. Ashouri, H.; Hsu, K.-L.; Sorooshian, S.; Braithwaite, D.K.; Knapp, K.R.; Cecil, L.D.; Nelson, B.R.; Prat, O.P. PERSIANN-CDR: Daily precipitation climate data record from multisatellite observations for hydrological and climate studies. *Bull. Am. Meteorol. Soc.* **2015**, *96*, 69–83. [CrossRef]
31. Prakash, S. Performance assessment of CHIRPS, MSWEP, SM2RAIN-CCI, and TMPA precipitation products across India. *J. Hydrol.* **2019**, *571*, 50–59. [CrossRef]
32. Sadeghi, M.; Nguyen, P.; Naeini, M.R.; Hsu, K.; Braithwaite, D.; Sorooshian, S. PERSIANN-CCS-CDR, a 3-hourly 0.04° global precipitation climate data record for heavy precipitation studies. *Sci. Data* **2021**, *8*, 1–11. [CrossRef] [PubMed]
33. Xie, P.; Arkin, P.A. An intercomparison of gauge observations and satellite estimates of monthly precipitation. *J. Appl. Meteorol. Climatol.* **1995**, *34*, 1143–1160. [CrossRef]
34. Darand, M.; Amanollahi, J.; Zandkarimi, S. Evaluation of the performance of TRMM Multi-satellite Precipitation Analysis (TMPA) estimation over Iran. *Atmos. Res.* **2017**, *190*, 121–127. [CrossRef]
35. Javanmard, S.; Yatagai, A.; Nodzu, M.; BodaghJamali, J.; Kawamoto, H. Comparing high-resolution gridded precipitation data with satellite rainfall estimates of TRMM_3B42 over Iran. *Adv. Geosci.* **2010**, *25*, 119–125. [CrossRef]

36. Deng, P.; Zhang, M.; Guo, H.; Xu, C.; Bing, J.; Jia, J. Error analysis and correction of the daily GSMaP products over Hanjiang River Basin of China. *Atmos. Res.* **2018**, *214*, 121–134. [CrossRef]
37. Guo, H.; Chen, S.; Bao, A.; Behrangi, A.; Hong, Y.; Ndayisaba, F.; Hu, J.; Stepanian, P.M. Early assessment of integrated multi-satellite retrievals for global precipitation measurement over China. *Atmos. Res.* **2016**, *176*, 121–133. [CrossRef]
38. Hırca, T.; Türkkan, G.E.; Niazkar, M. Applications of innovative polygonal trend analyses to precipitation series of Eastern Black Sea Basin, Turkey. *Theor. Appl. Climatol.* **2022**, *147*, 651–667. [CrossRef]
39. Tan, J.; Petersen, W.A.; Tokay, A. A novel approach to identify sources of errors in IMERG for GPM ground validation. *J. Hydrometeorol.* **2016**, *17*, 2477–2491. [CrossRef]
40. Tan, X.; Yong, B.; Ren, L. Error features of the hourly GSMaP multi-satellite precipitation estimates over nine major basins of China. *Hydrol. Res.* **2018**, *49*, 761–779. [CrossRef]
41. Gupta, M.; Srivastava, P.K.; Islam, T.; Ishak, A.M.B. Evaluation of TRMM rainfall for soil moisture prediction in a subtropical climate. *Environ. Earth Sci.* **2014**, *71*, 4421–4431. [CrossRef]
42. Gadouali, F.; Messouli, M. Evaluation of multiple satellite-derived rainfall products over Morocco. *Int. J. Hydrol. Sci. Technol.* **2020**, *10*, 72–89. [CrossRef]
43. Hu, Z.; Hu, Q.; Zhang, C.; Chen, X.; Li, Q. Evaluation of reanalysis, spatially interpolated and satellite remotely sensed precipitation data sets in central Asia. *J. Geophys. Res. Atmos.* **2016**, *121*, 5648–5663. [CrossRef]
44. Shayeghi, A.; Azizian, A.; Brocca, L. Reliability of reanalysis and remotely sensed precipitation products for hydrological simulation over the Sefidrood River Basin, Iran. *Hydrol. Sci. J.* **2020**, *65*, 296–310. [CrossRef]
45. Kawo, N.S.; Hordofa, A.T.; Karuppannan, S. Performance evaluation of GPM-IMERG early and late rainfall estimates over Lake Hawassa catchment, Rift Valley Basin, Ethiopia. *Arab. J. Geosci.* **2021**, *14*, 1–14. [CrossRef]
46. Wang, L.; Chen, R.; Song, Y. Research review on calculation methods and influential factors on areal precipitation of alpine mountains. *Plateau Meteorol.* **2017**, *36*, 1546–1556.
47. Goodarzi, M.R.; Sabaghzadeh, M.; Mokhtari, M.H. Impacts of aspect on snow characteristics using remote sensing from 2000 to 2020 in Ajichai-Iran. *Cold Reg. Sci. Technol.* **2022**, *204*, 103682. [CrossRef]